RSC Advances

ROYAL SOCIETY OF CHEMISTRY

www.rsc.org/advances

Journal Name

RSCPublishing

ARTICLE

Surface Modification of Poly (Propylene Carbonate) by Layer-by-Layer Assembly and its Hemocompatibility

Man Xi,[ab] Jing Jin,[b*] and Bao-yan Zhang[a*]

Cite this: DOI: 10.1039/xoxxoooooox

Received ooth January 2012,
Accepted ooth January 2012

DOI: 10.1039/xoxxoooooox

www.rsc.org/

Polyelectrolyte multilayers of negative charged heparin (Hep) and positive charged lysozyme (LYZ) were used to immobilize on poly (propylene carbonate) (PPC) surface by layer-by-layer (LbL) assembly to improve hemocompatibility. X-ray photoelectron spectroscopy confirmed that the surface was successfully modified. The process of LbL and the subsequent fibrinogen adsorption was monitored by quartz crystal microbalance with dissipation in real time. The adsorbed fibrinogen on the PPC surface formed dense side-on structures, which was leading to lots of platelet adhesion. However, on the surface of PPC-g-(LYZ-co-Hep)$_3$, fibrinogen molecules formed a relatively loose adsorbed layer, which had an excellent fibrinogen resistance by release of dissipated energy. Combined with the results of platelet adhesion, erythrocyte adhesion, and hemolysis, we concluded that PPC-g-(LYZ-co-Hep)$_3$ surface had high performance with hemocompatibility by highly hydrophilicity of LYZ and anticoagulation of Hep, which can be as a candidate scaffold material for blood vessel tissue engineering.

1. Introduction

Poly (propylene carbonate) (PPC) is a kind of aliphatic polycarbonate copolymerized from carbon dioxide and propylene oxide at the end of the 1960s with a rudimentary catalyst based on water and diethyl zinc[1]. It is biodegradable and can be used as adhesives, photoresists, barrier materials, and biomaterials[2, 3]. In vivo degradation of PPC had been monitored for use as a surgical polymer, or as slow-release substrate[4]. In addition, PPC can be considered as an alternative to polycaprolactone in tissue engineering due to its acceptable mechanical strength and biocompatibility[5]. Zhao et al. fabricated a biomimetic PPC porous scaffold with nanofibrous chitosan network within macrospores, which was a potential candidate for bone tissue engineering[6]. Zhang et al. reported that PPC were blended with poly (3-hydroxybutyrate-co-3-hydroxyhexanoate) by solvent casting method to obtain scaffold material for blood vessel tissue engineering[7]. However, the major drawback of PPC in blood vessel scaffold is its surface hydrophobicity and poor hemocompatibility. Thus, it is significant to enhance hemocompatibility of PPC surface, including antifouling properties, anti-platelet activation, and anti-hemolysis[8].

Several methodologies have been used to modify polymer surfaces, such as gamma ray irradiation[9], plasma discharge[10], and ultraviolet-induced graft polymerization[11]. Layer-by-layer (LbL) technique is a simple and versatile method for fabricating organized assemblies functional thin films on solid substrate[12, 13]. Generally, LbL films are made of the oppositely charged polycations and polyanions by electrostatic interactions[14]. Dehghani et al. used polyethylenimine/gelatin LBL assembly techniques combination of aminolysis to modify PPC surface. The modified PPC with three bilayers assembly was remarkably promoted both fibroblast and primary human osteoblasts cell attachment, spreading and growth5. Numerous studies have focused on improving the hemocompatibility of biomaterial by LbL[15-17]. Brynda and Houska used LbL for preparation of hemocompatible coating, such as bovine serum albumin/poly (L-lysine)[18] and albumin/heparin(Hep)[19] based on hydrophobic and electrostatic interactions. Collagen and sulfated chitosan multilayers were coated on pure titanium using a LbL self-assembly technique[20] for excellent anticoagulation properties in vitro. Thus, surface modification of PPC with LbL assembly is an effective method for improving its hemocompatibility, especially protein adsorption[21], platelet adhesion[22], and red blood cell (RBC) attachment[23].

Grafting biomacromolecules, such as polysaccharides and proteins, to surfaces is attractive because those different biomacromolecular components had synergic property by the

interpenetration on a multilayer surface[24]. Lysozyme (LYZ) is a small monomeric globular enzymatic protein with 129 amino acids cross-linked by four disulfide bridges[25]. It holds an excess of 8 positive charges under physiological condition[26] and has high hydrophilicity. Hep is an efficient nature anticoagulant that contains sulfuric, sulfo-amino and carboxyl groups, which is a polydispersed anionic polysaccharide molecule with a molecular weight ranging between 6000 and 35,000[27]. Immobilizing Hep to surfaces in vitro has been proved to prevent thrombus formation[28], improve hemocompatibility of blood-contacting biomaterials[29], and reduce activation of complement and blood cells[30]. Thus, immobilizing Hep and LYZ on the surface can fabricate hemocompatible material with high hydrophilicity and anticoagulation.

In this study, polyelectrolyte multilayers of negative charged Hep and positive charged LYZ were used to immobilize on the surface of PPC by LbL assembly to improve the hemocompatibility. The multilayers were stabilized by crosslinking the amino groups of LYZ and heparin with glutaraldehyde. The hemocompatibility of modified membranes were evaluated in terms of protein adsorption, platelet adhesion, RBC adhesion, and hemolysis assays. In addition, the process of LbL and the subsequent fibrinogen adsorption was monitored by QCM-D in real time.

2. Experimental

2.1 Materials

Poly (propylene carbonate) (PPC) is obtained from Changchun Institute of Applied Chemistry, China. The weight-average molecular weight (Mw) was 1.0× 105 and molecular mass dispersity was 1.23. The elastic modulus and elongation at break of PPC is 56.4MPa and 612.25%, respectively. The PPC was precipitated from 5 wt. % PPC/dichloromethane solution with a large excess of methanol (with hydrochloric acid 1wt.%)[31]. PPC membrane was prepared as follows: PPC (1 g) was dissolved in 50 mL of dichloromethane at 25℃. The homogeneous solutions obtained were slowly dropped onto a glass plate and dried in vacuum for 12h at room temperature to a constant weight. The membrane was cleaned with ethanol/water (1/1, v/v) solution for 1 h, followed by rinsing with of deionized water, and then dried under vacuum for 24 h at room temperature before use. Heparin sodium salt, lysozyme (LYZ) and fibrinogen (Fib) were obtained from Sigma Chemical Co. Phosphate buffered saline (PBS 0.9% NaCl, 0.01 M phosphate buffer, pH 7.4) used for protein adsorption, platelet adhesion and QCM-D experiment was prepared freshly. All other reagents were of AR grade and used without further purification.

2.2 Preparation of PPC multilayer membranes by layer-by-layer assembly

PPC membrane (2cm × 2cm) was immersed into LYZ (5mg/ml) in PBS solution at 50℃ for 24h agitating at 150rpm. The LYZ was grafted onto PPC surface by aminolysis reaction. Then, the membrane was rinsed by PBS three times. The scheme of layer-by-layer assembly of surface modification of PPC-g-LYZ is shown in Fig. 1. After grafting LYZ onto the surface of PPC, the positive charged surface was immersed in a heparin PBS solution (pH 7.4) for 20min at 20℃, followed by PBS rinsed three times. Afterward, the membrane was immersed into a 1mg/mL solution of LYZ (pH 7.4) for 20min. After washing with PBS, the membrane was immersed into heparin again and rinsed with PBS. And then, the multilayer of PPC-g-(LYZ-co-Hep)$_3$ was formed on the surface of PPC by repeating this procedure several times. Finally, the modified PPC membrane was fixed by 5 mg/mL glutaraldehyde solution for 20 min, rinsing with PBS solution and drying in a vacuum oven at room temperature.

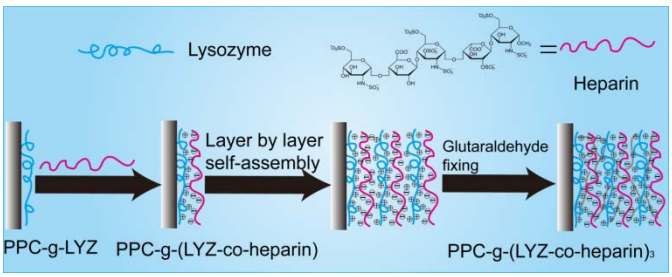

Fig. 1 Schematic diagram illustration of the surface modification of PPC membranes by layer-by-layer assembly.

2.3 Surface characterization

Surface composition of PPC and modified PPC membranes were analysed via X-ray photoelectron spectroscopy (XPS, VG Scientific ESCA MK II Thermo Advantage V 3.20 analyzer) with Al/K (hν= 1486.6 eV) anode mono-X-ray source at the detection angle of 90°. Surface spectra were collected over a range of 0–1200 eV and higher solution spectra of C1s, O1s, N1s, and S2p regions were provided. The graft concentration of the different samples was determined by peak–area ratios. The water static contact angles of pristine and modified membrane were assessed by sessile drop water angle measurement using a contact angle goniometer (DSA 100, KRÜSS GmbH, Hamburg, Germany) by placing 2 μ L of distilled water on the surfaces at 25℃. Six parallel experiments were made on a single sample to obtain the average value of contact angle.

2.4 Blood compatibility test

2.4.1 Platelet adhesion test

Fresh blood collected from a healthy rabbit was immediately mixed with a 3.8 wt.% solution of sodium citrate at a dilution ratio of 9:1 (blood: sodium citrate solution). The diluted blood was performed in all blood compatibility tests. The blood was centrifuged at 1000 rpm for 10 min at 8°C to obtain the platelet-rich plasma (PRP). The membrane (1 cm×1 cm) was introduced with 100 μL PRP, and then incubated at 37 °C for 2 h under a static state. After incubation, the membrane was again rinsed with PBS three times to remove any non-adhering platelets. The membrane was transferred to new wells. Subsequently, the membrane was immersed in PBS solution containing 2.5wt.% glutaraldehyde for 8 h at 4°C to set the adhered platelets. After thorough washing with deionized water three times, the platelets were dehydrated with 30%, 50%, 70%, 90%, and 100%(v/v) ethanol/water solution for 30min each in

sequence, and then naturally dried in the air. A sample was then gold sputtered in vacuum and observed by field-emission scanning electron microscopy (FESEM, XL 30 ESEM FEG, FEI Company)[32].

2.4.2 Erythrocyte adhesion

Fresh blood collected from a healthy rabbit was mixed immediately with a 3.8 wt.% solution of sodium citrate at a dilution ration of 9:1. (The experiments were carried out in accordance with the guidelines issued by the Ethical Committee of the Chinese Academy of Sciences). Erythrocytes were separated from plasma and lymphocytes by centrifugation (3000g, 5 min) at 4℃, washed three times with normal saline and suspended in normal saline. Erythrocytes were used immediately after isolation. Diluted red blood cell solution contained 10% fresh anticoagulated rabbit RBC and 90% physiological salt solution. Pristine and modified PPC membranes of pieces (1 cm×1 cm) were incubated for 2 h in PBS and placed in a tissue culture plate. Then 2 mL of diluted RBC solution was placed on the substrate surface in each well of the tissue culture plate for 60 min at 37 ℃. After the membranes were washed with PBS, blood cells adhering to the film were fixed by 2.5 wt. % glutaraldehyde at 4℃ for 10 h. Finally, the membranes were washed with PBS three times, and dehydrated with a series of ethanol/water mixtures (30, 50, 70, 90, and 100 vol. % ethanol; 30 min in each mixture). The surface of the membrane was gold sputtered in vacuum and observed with field emission scanning electron microscopy (SEM, FESEM, XL 30 ESEM FEG, FEI Company).

2.4.3 Hemolysis rate

The membrane (1cm×1cm) was immersed in diluted blood solution containing 5% fresh anticoagulated rabbit blood and 95% physiological salt solution, and then incubated at 37°C for 2h, 6h, and 12h. After centrifugation at 3000 rpm for 20 min, the absorbance of the solution was recorded as D_t. Under similar conditions, the solution containing 5% fresh anticoagulated rabbit blood and 95% physiological salt solution was used as negative reference, whereas the solution containing 5% fresh anticoagulated rabbit blood and 95% distilled water was used as positive reference. This absorbance was recorded as D_{nc} and D_{pc}, respectively. The hemolysis rate α of the films was calculated using the following formula[33]:

$$\alpha(\%) = \frac{D_t - D_{nc}}{D_{pc} - D_{nc}} \times 100 \quad (1)$$

2.5 Quartz crystal microbalance with dissipation (QCM-D)

QCM-D procedure was performed to record the layer-by layer process to PPC surface and fibrinogen adsorption process (QCM-D E4, Q-sense AB, Gothenburg, Sweden). The AT-cut piezoelecteic quartz crystal disks coated with gold used as the QCM-D sensor chips (Q-sense Biolin Scientific AB, Sweden) had the fundamental frequency of 4.95MHz and vibrate in the thickness-shear mode with the overtone n of 1, 3, 5, 7, 9, 11, and 13. QCM-D chip was exposed to UV-lamp (185nm+254nm) for 15min to remove organic contaminants, and then was cleaned in a 5:1:1 (v/v) solution of deionized water, ammonia (25%) and hydrogen peroxide (30%) for 5min at 75℃[34]. Finally the crystals were washed with deionized water and dried under a flow of nitrogen. 2wt.% PPC in dichloromethane solution was spin-coated onto the crystals with 2500rpm for 20s. The film was dried with the sensor in vacuum for 12h.

After grafting LYZ using the same process as before, the crystal was placed in the QCM-D module. The QCM-D cell was thoroughly rinsed with PBS buffer between each measurement. After stabilization of the baseline in PBS, heparin in PBS was injected with a concentration of 1mg/mL for 15min, thus an electrostatic interaction layer was formed on the sensor. Thereafter, LYZ protein was injected with1 mg/mL in PBS for 15min, and then injected heparin as before. Repeated the same procedure and the multilayer of PPC-g-$(LYZ\text{-co-}Hep)_3$ were formed on the sensor. Finally, glutaraldehyde PBS solution with 5 mg/mL was injected into the chamber for 30min, and then rinsed by PBS. In QCM-D experiment, the temperature was controlled at 20℃ (±0.02℃) and the flow rate was fixed at 50 uL min^{-1}. For each condition, the experiments were repeated multiple times. A representative data set was then presented.

The change of adsorbed fibrinogen mass produced shifts of the frequency and the viscoelasticity variation of the adsorbed layer could induce the dissipation variation. It is necessary to use the Voigt model to calculate adsorbed mass of fibrinogen[35]. Voigt model is a common model to be used to describe the polymer's viscoelasticity property. The model contains a spring and a dashpot as its elements to represent the elastic (storage) and inelastic (damping) behaviour of a material, respectively[36]. Using this model in our fitting process, each layer is represented by four unknown parameters: layer density ρ (kg m^{-3}), layer viscosity η (or G''/ω, kg ms^{-1}), layer shear modulus μ (or G', Pa) and layer thickness σ (m)[37]. The frequency shift Δf and the dissipation shift ΔD recording by QCM-D real-time have the relationship with those parameters as follows[38, 39]:

$$\Delta f = f_1(n, \eta_f, \rho_f, \mu_f, \sigma_f) \quad (2)$$

$$\Delta D = f_2(n, \eta_f, \rho_f, \mu_f, \sigma_f) \quad (3)$$

$$G^* = G' + jG'' = \mu + j2\pi f\eta \quad (4)$$

In our fitting process, overtones n= 3, 5, 7, 9, 11, 13 were used, allowing the model to fit the data and calculate the four unknown parameters $(\eta, \rho, \mu, \sigma)$ by iterating using QTools software (Q-Sense). Adsorbed layer density was assumed as 1200kg/m^3 (consider the layer density value between the banding water density 1000kg/m^3 and protein density 1400kg/m^3)[40]. The density and viscosity of the liquid phase were set as 1000kg/m^3 and 0.001kg/ms, respectively. The density of the each layer was iterated to find a suitable value then fixed in. The parameters of the layer viscosity, layer shear modulus and layer thickness were set in the range of

0.0001~0.1kg/ms, 1×10^{5}-1×10^{7}Pa, 1×10^{-11}-1×10^{-6}m, respectively[41].

3. Results and discussion

3.1 Surface characterization of modified PPC

The surface chemical compositions of PPC-g-LYZ and PPC-g-(LYZ-co-Hep)$_3$ are confirmed by XPS analysis. Fig. 2 shows the XPS spectra of PPC and modified PPC from binding energy 0-600 eV. After grafting of LYZ, the appearance of N1s binding energy at 400 eV in the wide scan of PPC-g-LYZ spectra, confirmed the presence of LYZ on the surface of PPC. The chemical composition and atomic concentration of pristine PPC and modified PPC surfaces are listed in Table 1. The carbon and oxygen atomic concentration of PPC is the average value of the top and bottom surfaces. First, the top (air surface) and bottom (glass surface) of PPC may have different degradation rates. Second, the dispersity of the employed PPC film obtained by solvent casted may be heterogeneous with surface enriched, which can lead to the difference of top and bottom[42]. The oxygen atomic concentration decreases and the nitrogen atomic concentration increases up to 6.67%. After layer-by-layer assembly, LYZ and heparin were anchored onto the surface of PPC. Since the elemental ratio of heparin is approximately C: O: N: S = 12:14:2:1, the additional N1s (binding energy 400eV) and S2p peak (binding energy 167eV) in the spectrum of PPC-g-(LYZ-co-Hep)$_3$ surface is observed, which suggests that the heparin has been grafted onto PPC surface. In Table 1, both the oxygen and nitrogen atomic concentrations sharply increase. This is because that heparin is a kind of sulfated polysaccharide that contains sulfuric, sulfo-amino and carboxyl groups. All of these results prove that LYZ and heparin are successfully immobilized onto the surface of PPC.

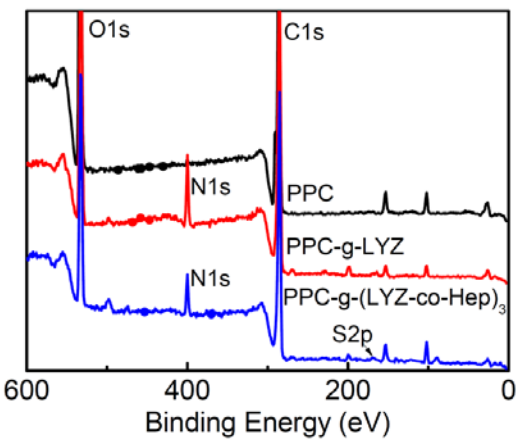

Fig. 2 XPS wide scan spectra of pristine PPC, PPC-g-LYZ, and PPC-g-(LYZ-co-Hep)$_3$.

Table 1. Surface elemental compositions of the membranes from XPS analysis.

Samples	Compositions (at.%)			
	C (%)	O (%)	N (%)	S (%)
PPC	65.49	34.51	-	-
PPC-g-LYZ	67.95	25.38	6.67	-
PPC-g-(LYZ-co-Hep)$_3$	45.62	41.64	10.32	2.42

Fig. 3 shows static water contact angle of the pristine PPC and modified PPC. The water contact angle of PPC is nearly 80°, whereas that of the PPC-g-LYZ and PPC-g-(LYZ-co-Hep)$_3$ is 61° and 43°, respectively. When PPC membrane is reacted with LYZ by aminolysis, the membrane shows a bit lower contact angle than that of the pristine PPC, implying an improvement of hydrophilicity. The inactivated LYZ at 50℃ endows hydrophilic amino acids are exposed to the outer environment, whereas hydrophobic amino acids reside at the PPC interface[43]. The denatured proteins as a primary step for further modification with functional groups had been reported by Genzer et al[44]. After further modification with layer-by-layer assembly, the water contact angle decreases, which is attributed to the introduction of a lot of polar compositions[45].

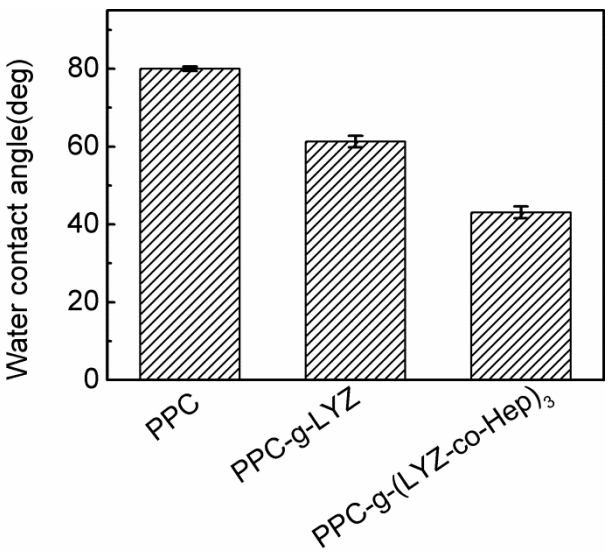

Fig. 3 Water contact angle of pristine PPC, PPC-g-LYZ, and PPC-g-(LYZ-co-Hep)$_3$.

3.2 Layer-by-layer assembly of LYZ/heparin on the surface of PPC by QCM-D

The detail of layer-by-layer assembly of LYZ/heparin determined by QCM-D on the surface of PPC is described in Fig. 4. The sequential LbL deposition of oppositely charged polyelectrolytes on a solid surface results in a polyelectrolyte multilayer. Cycle 1 represented that heparin was injected onto the positive surface of PPC-g-LYZ. The frequency decreased and dissipation increased, indicating heparin was immobilized onto the sensor by electrostatic interaction with LYZ and viscoelastic of film increased. In cycle 2, LYZ and heparin was injected, subsequently. After heparin was injected, a sharp peak appeared in frequency and dissipation shifts figures and the same phenomenon was shown in cycle 3. This suggested that

the heparin molecule was sharply immobilized onto the surface by electrostatic interaction at the initial stage and a relatively loose multilayer was form on the surface[45]. Combined with heparin was injected further, a small part of LYZ/heparin combination was rinsed, which confirmed by the change of dissipation. The glutaraldehyde is a cross-linker because it forms linkages with both the amine and carboxylic groups of LYZ and heparin. After fixing the multilayers by glutaraldehyde, followed by PBS rinsed, the frequency and dissipation tended to steady. Thus, a stable multilayer by LbL was form on the surface of PPC. In the system of LYZ/heparin, the deposited LYZ can induce the adsorption of fibrinogen and platelet adhesion. Thus, the total amount of heparin in the LBL assembly of LYZ/heparin is significant for the improvement of hemocompatibility[19]. The cycles can be repeated until the content of heparin up to screening out the positively charged effect of LYZ. Elemental sulphur can be used to calculate the degree of heparin surface coverage on the modified PPC surface[11]. The theoretical value of sulphur atomic percentage in heparin is 3.44%. The sulphur atomic percentage determined by XPS on the 3 cycles modified PPC surface is 2.42%, which means the surface coverage of heparin is up to 70.3%. The high surface coverage of heparin endows PPC with protein resistance and anticoagulant activity.

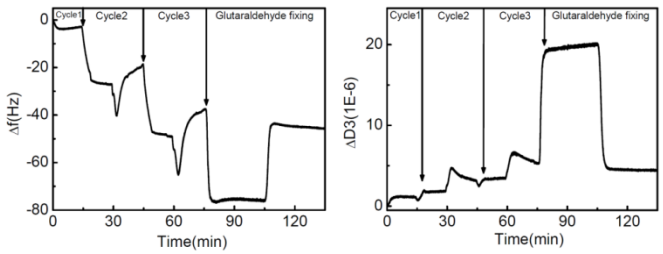

Fig. 4 Frequency and dissipation shifts of the PPC-g-(LYZ-co-Hep)$_3$ film as measured by QCM-D.

3.3 Fibrinogen adsorption by QCM-D

Fig. 5 shows the frequency shift ($\triangle f$) and dissipation shift ($\triangle$D) in QCM-D measurement of adsorption of fibrinogen in real time on different PPC surfaces. The fitting masses of adsorbed proteins are shown in Table 2. In general, an increase in -$\triangle f$ indicates an increase in the coupled mass to the quartz crystal, whereas an increase in $\triangle D$ indicates increased viscous loss to the adsorbed layers. After fibrinogen protein solution is added, $\triangle f$ decreases and $\triangle D$ sharply increases, indicating that the fibrinogen molecules are adsorbed on the PPC surface. After then, $\triangle f$ and $\triangle$ D gradually level off, implying the saturation of adsorption. The adsorbed fibrinogen mass on the PPC surface is 170±8 ng cm^{-2} (Table 2), which suggests that fibrinogen has an intense hydrophobic interaction on the PPC surface. For PPC-g-LYZ, after fibrinogen is added, $\triangle f$ decreases and $\triangle D$ gradually increases, implying that fibrinogen molecules are slowly adsorbed on the surface of PPC-g-LYZ by electrostatic interaction. While on the surface of PPC-g-(LYZ-co-Hep)$_3$, $\triangle f$ slightly decreases and $\triangle D$ sharply increases at the first injecting of fibrinogen, which indicating that a few fibrinogen molecules are adsorbed on the surface of PPC-g-(LYZ-co-Hep)$_3$. This generates a relatively loose adsorbed layer that can be easily rinsed. After then, $\triangle f$ increases and $\triangle D$ gradually decreases to almost zero, suggesting that PPC-g-(LYZ-co-Hep)$_3$ surface has protein resistance due to hydrophilicity of LYZ and anticoagulation of Hep. In addition, the fibrinogen adsorbed mass on the surface of PPC-g-LYZ and PPC-g-(LYZ-co-Hep)$_3$ are 52±5 and 11±3 ng cm^{-2}, respectively. This also proves that PPC-g-(LYZ-co-Hep)$_3$ surface has excellent fibrinogen resistance. Fibrinogen is a rodlike protein with the dimension of 47 nm×5 nm ×5 nm[47], which plays an important role in coagulation, platelet adhesion. The theoretical adsorption amounts of fibrinogen on a surface in the side-on and end-on close-packed monolayer surface coverage are 240 ng cm^{-2} and 2260 ng cm^{-2}, respectively[48]. Thus, fibrinogen molecules form dense side-on structures on the surface of PPC because of strong hydrophobic interactions, which can induce platelet adhesion and thrombus formation. However, fibrinogen molecules form a relatively loose adsorbed layer on the surface of PPC-g-(LYZ-co-Hep)$_3$, which is easily rinsed by the subsequent fibrinogen injecting and PBS. This can be proved by the relationship of $\triangle f$ and $\triangle D$ when fibrinogen molecules adsorb on the surface of fibrinogen adsorption onto the surface of PPC and PPC-g-(LYZ-co-Hep)$_3$ (Fig. 6). After fibrinogen was injected, the change of $\triangle f$ was nearly not obvious but $\triangle D$ had a great change, which indicated that the surface of PPC-g-(LYZ-co-Hep)$_3$ resisted fibrinogen adsorption by release of dissipation energy. In addition, the relationship of $\triangle f$ and $\triangle D$ on the surface of PPC increase monotonously, whereas on the surface of PPC-g-(LYZ-co-Hep)$_3$ presented a closed loop, eventually returned to the origin site. However, this origin is not the site before fibrinogen injected. A part of energy was released to suppress the protein adsorption. Therefore, PPC-g-(LYZ-co-Hep)$_3$ surface may have an excellent fibrinogen resistance by release of dissipated energy.

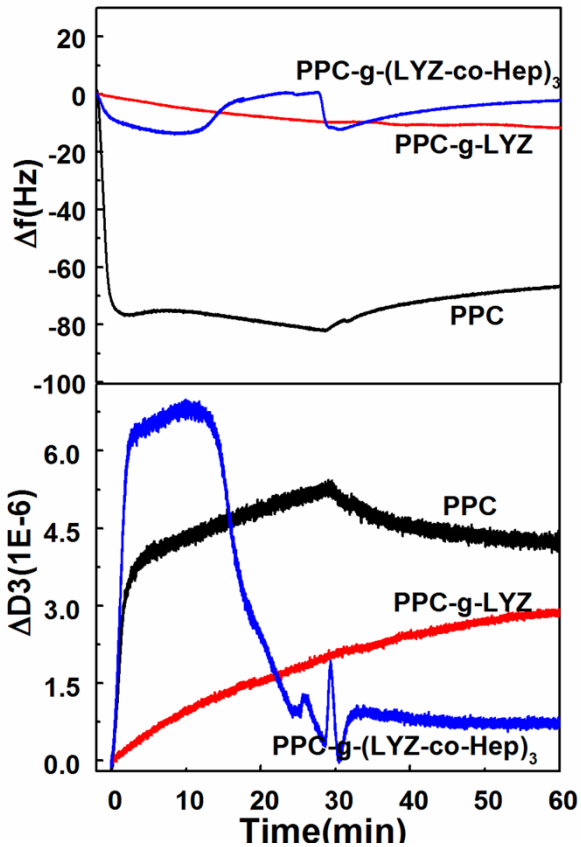

Fig. 5 The frequency shift (Δf) and dissipation shift (ΔD) in QCM-D measurement of the adsorption of fibrinogen on the surfaces of PPC, PPC-g-LYZ, and PPC-g-(LYZ-co-Hep)$_3$.

Table 2. Overview of adsorbed fibrinogen frequency and dissipation changes and the fitting mass of PPC, PPC-g-LYZ, and PPC-g-(LYZ-co-Hep)$_3$.

Samples	Frequency (Hz)	Dissipation(1E-6)	Mass (ng cm^{-2})
PPC	67.3±0.5	4.3±0.1	170±8
PPC-g-LYZ	11.3±0.2	2.8±0.4	52±5
PPC-g-(LYZ-co-Hep)$_3$	2.5±0.3	0.7±0.1	11±3

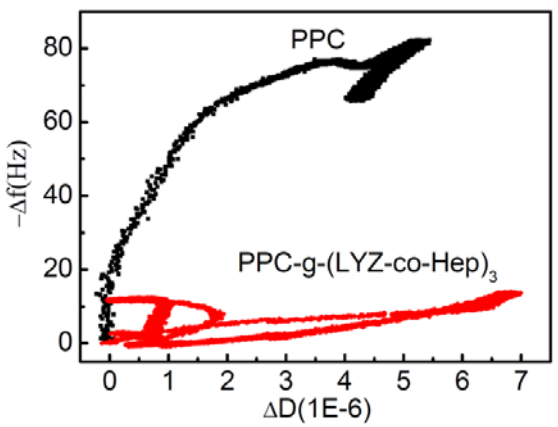

Fig.6 ΔD vs. Δf relation of fibrinogen adsorption onto the surface of PPC and PPC-g-(LYZ-co-Hep)$_3$.

3.4 Platelet adhesion

When a surface is exposed to blood, plasma proteins are rapidly adsorbed on the surface, followed by platelet adhesion and activation, coagulation, complement activation, and other blood cell responses[49, 50]. Fig. 7 shows SEM pictures of platelet adhered on the surface of PPC and modified PPC. A large amount of platelets adhered on the pristine PPC surface, exhibiting highly activated with spread and pseudopodia states because of the hydrophobic property of PPC. The number of platelet adhered on the surface of PPC-g-LYZ decreased and the state of adhered platelet maintained round shape. The existence of platelets on PPC-g-LYZ surface is because the electrostatic interaction between positive charged LYZ and negative charged platelet in physiological condition. However, nearly no platelet adhered on the surface of PPC-g-(LYZ-co-Hep)$_3$, except some small platelet fragments. Thus, the excellent hemocompatibility of PPC-g-(LYZ-co-Hep)$_3$ is due to the highly hydrophilic surface property and the anticoagulation of Hep. In addition, the process of platelet adhesion is controlled by protein adsorption, especially fibrinogen adsorption. The results of fibrinogen adsorption by QCM-D has proved that the surface of PPC-g-(LYZ-co-Hep)$_3$ can efficiently suppress the approach of fibrinogen, and then disrupted the interaction between RGD and dodecapeptide sequences in fibrinogen and GPIIb/IIIa integrin, which is the receptor on the platelet surface[51], leading to few platelets adhesion.

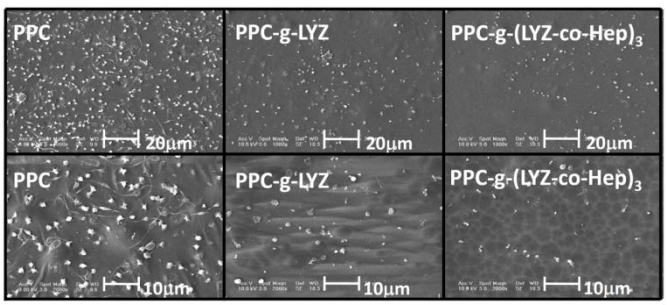

Fig. 7 SEM images of platelets adhered on the surfaces of pristine PPC, PPC-g-LYZ, and PPC-g-(LYZ-co-Hep)$_3$.

3.5 Erythrocyte adhesion

Different from platelets adhesion, the transmembrane proteins involved in the regulation and signal transduction in RBC are non-adherent[52]. Interaction of RBCs with surfaces includes van der Waals interactions, electrostatic forces, bending undulations, and steric effects[53, 54]. Fig. 8 shows the erythrocyte adhesion of pristine PPC, PPC-g-LYZ, and PPC-g-(LYZ-co-Hep)$_3$. Similar with platelet adhesion of PPC, the number of erythrocyte adhesion on the surface of PPC is the largest because of the hydrophobicity of PPC. Some echinocytes are observed on PPC surface, lost their normal shapes, whereas erythrocytes maintained their normal discoid shapes and sizes on the surfaces of PPC-g-LYZ and PPC-g-(LYZ-co-Hep)$_3$. There were no significant differences in PPC-g-LYZ and PPC-g-(LYZ-co-Hep)$_3$, which is because that the erythrocyte adhesion is controlled by the non-adherent transmembrane proteins. Combined with the data of platelet

and erythrocyte adhesion, we concluded that the PPC-g-(LYZ-co-Hep)$_3$ surface had high-performance of anticoagulation.

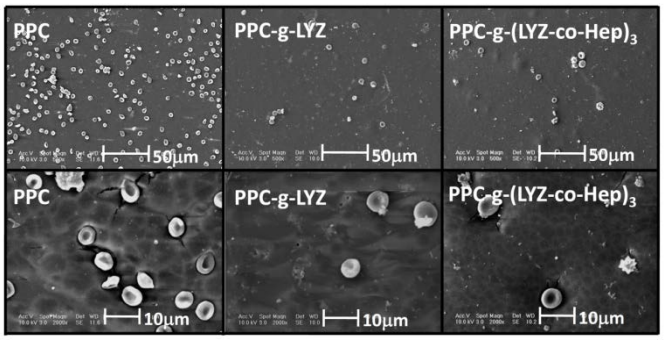

Fig. 8 SEM images of RBC adhered on the surfaces of pristine PPC, PPC-g-LYZ, and PPC-g-(LYZ-co-Hep)$_3$.

3.6 Hemolysis assay

Hemolysis assay is an important parameter for evaluating blood compatibility. The research on biomaterial surface-induced hemolysis is significantly neglected, especially hemolysis during RBCs storage and transportation. The hemolysis ratio represents the extent of the RBC rupture caused by the release of hemoglobin. The hemolysis ratios of PPC and modified PPC are shown in Fig. 9. At the initial stage of interacting with RBC suspension (2h and 12h), there is no obvious difference among the three samples. This is because that RBC is a suspension cell and hardly contacts with surface at the initial stage. After 24h, the hemolysis of PPC-g-(LYZ-co-Hep)$_3$ is lower than that of the other samples, which implying that the LbL modified PPC resist hemolysis and protect the morphology of RBC at long time contact. Therefore, we conclude that the PPC-g-(LYZ-co-Hep)$_3$ has high performance with hemocompatibility for suppressing platelet adhesion, RBC adhesion, and hemolysis.

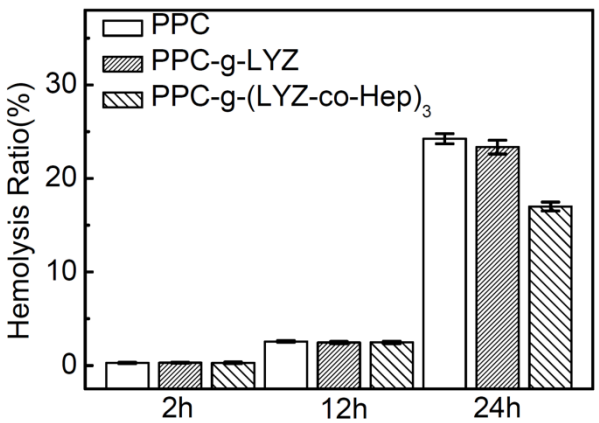

Fig. 9 Hemolysis rates of PPC and modified PPC at different times.

4. Conclusions

The surface modification of PPC was fabricated with negative charged Hep and positive charged LYZ by LbL. The process of LbL and the subsequent fibrinogen adsorption was monitored by QCM-D in real time, which indicated that the adsorbed fibrinogen on the surface of PPC formed dense side-on structures, leading to a number of platelet adhesion, whereas on the surface of PPC-g-(LYZ-co-Hep)$_3$, fibrinogen molecules formed a relatively loose adsorbed layer, which had an excellent fibrinogen resistance by release of dissipated energy. Furthermore, the results of platelet adhesion, erythrocyte adhesion, and hemolysis proved that the PPC-g-(LYZ-co-Hep)$_3$ had high performance with hemocompatibility by hydrophilicity of LYZ and anticoagulation of Hep, which can be as a candidate scaffold material for blood vessel tissue engineering. Last but not least, a lower elastic modulus and a higher percentage of elongation at break of PPC presented promise in application as a candidate scaffold material for blood vessel tissue engineering.

Acknowledgements

The authors acknowledge the financial support of the National Natural Science Foundation of China (Project No. 51303178).

Notes and references

[a] The Research Center for Molecular Science and Engineering, Northeastern University, Shenyang 110819, P. R. China; E-mail: byzhang2005@126.com

[b] State Key Laboratory of Polymer Physics and Chemistry, Changchun Institute of Applied Chemistry, Chinese Academy of Sciences, Changchun 130022, P. R. China; E-mail: jjin@ciac.ac.cn; Fax: +86-431-85262126; Tel: +86-431-85262971

1. S. Inoue, H. Koinuma and T. Tsuruta, *J. Polym. Sci. Pol. Lett.*, 1969, **7**, 287-292.
2. L. B. Chen, S. Y. Yang, X. X. Lin, S. Liu, D. S. Wang, A. F. Yu and S. J. He, *Polym. Advan. Technol.*, 2001, **12**, 687-692.
3. H. Pang, B. Liao, Y. H. Huang and G. M. Cong, *J. Appl. Polym. Sci.*, 2002, **86**, 2140-2144.
4. G. A. Luinstra and E. Borchardt, in *Synthetic Biodegradable Polymers*, eds. B. Rieger, A. Kunkel, G. W. Coates, R. Reichardt, E. Dinjus and T. A. Zevaco, 2012, vol. 245, pp. 29-48.
5. X. Zhong, Z. Lu, P. Valtchev, H. Wei, H. Zreiqat and F. Dehghani, *Colloid Surface. B*, 2012, **93**, 75-84.
6. J. Zhao, W. Han, H. Chen, M. Tu, S. Huan, G. Miao, R. Zeng, H. Wu, Z. Cha and C. Zhou, *J. Mater. Sci-mater. M.*, 2012, **23**, 517-525.
7. L. Zhang, Z. H. Zheng, J. Xi, Y. Gao, Q. Ao, Y. D. Gong, N. Zhao and X. F. Zhang, *Eur. Polym. J.*, 2007, **43**, 2975-2986.
8. K. K. Goli, O. J. Rojas and J. Genzer, *Biomacromolecules*, 2012, **13**, 3769–3779.

9. S. H. Chen, Y. Chang, K. R. Lee, T. C. Wei, A. Higuchi, F. M. Ho, C. C. Tsou, H. T. Ho and J. Y. Lai, *Langmuir*, 2012, **28**, 17733-17742.
10. C. C. Ferraz, G. H. Varca, J.-C. Ruiz, P. S. Lopes, M. B. Mathor, A. B. Lugão and E. Bucio, *Radiat. Phys. Chem.*, 2014, **97**, 298-303.
11. C. Zhang, J. Jin, J. Zhao, W. Jiang and J. Yin, *Colloid Surface. B*, 2013, **102**, 45-52.
12. D.-d. Li, K.-f. Ren, H. Chang, H.-b. Wang, J.-l. Wang, C.-j. Chen and J. Ji, *Langmuir*, 2013, **29**, 14101-14107.
13. J. Zhao, X. Wang, Y. Kuang, Y. Zhang, X. Shi, X. Liu and H. Deng, *RSC Adv.*, 2014.
14. X. Huang, A. B. Schubert, J. D. Chrisman and N. S. Zacharia, *Langmuir*, 2013, **29**, 12959-12968.
15. W. Tong, X. Song and C. Gao, *Chem. Soc. Rev.*, 2012, **41**, 6103-6124.
16. L.-C. Su, Y.-H. Chen and M.-C. Chen, *ACS Appl. Mater. Interfaces*, 2013, **5**, 12944-12953.
17. M. Y. Zhao, L. H. Li, B. Li and C. R. Zhou, *Express Polym. Lett.*, 2014, **8**, 322-335.
18. E. Brynda, J. Pachernik, M. Houska, Z. Pientka and P. Dvorak, *Langmuir*, 2005, **21**, 7877-7883.
19. M. Houska, E. Brynda, A. Solovyev, A. Brouckova, P. Krizova, M. Vanickova and J. E. Dyr, *J. Biomed. Mater. Res. A*, 2008, **86A**, 769-778.
20. Q.-L. Li, N. Huang, J. Chen, G. Wan, A. Zhao, J. Chen, J. Wang, P. Yang and Y. Leng, *J. Biomed. Mater. Res. A*, 2009, **89A**, 575-584.
21. Y. Lvov, K. Ariga, I. Ichinose and T. Kunitake, *J. Am. Chem. Soc.*, 1995, **117**, 6117-6123.
22. M. Gong, Y.-B. Wang, M. Li, B.-H. Hu and Y.-K. Gong, *Colloid Surface. B*, 2011, **85**, 48-55.
23. J. Almodovar, L. W. Place, J. Gogolski, K. Erickson and M. J. Kipper, *Biomacromolecules*, 2011, **12**, 2755-2765.
24. Q. Lin, J. Van, F. Qiu, X. Song, G. Fu and J. Ji, *J. Biomed. Mater. Res. A*, 2011, **96A**, 132-141.
25. S. Li, J. J. Mulloor, L. Wang, Y. Ji, C. J. Mulloor, M. Micic, J. Orbulescu and R. M. Leblanc, *ACS Appl. Mater. Interfaces*, 2014, **6**, 5704-5712.
26. M. Boncina, J. Rescic and V. Vlachy, *Biophys. J.*, 2008, **95**, 1285-1294.
27. Y. Byun, H. A. Jacobs, J. Feijen and S. W. Kim, *J. Biomed. Mater. Res.*, 1996, **30**, 95-100.
28. K. Zhang, J.-A. Li, K. Deng, T. Liu, J.-Y. Chen and N. Huang, *Colloid Surface. B*, 2013, **108**, 295-304.
29. J. Chen, C. Chen, Z. Chen, J. Chen, Q. Li and N. Huang, *J. Biomed. Mater. Res. A*, 2010, **95A**, 341-349.
30. L. Nguyen Minh, Y. Teramura and H. Iwata, *Biomaterials*, 2011, **32**, 6487-6492.
31. C. Barreto, E. Hansen and S. Fredriksen, *Polym. Degrad. Stabil.*, 2012, **97**, 893-904.
32. F. Xu, Y. Li, E. Kang and K. Neoh, *Biomacromolecules*, 2005, **6**, 1759-1768.
33. G. Li, P. Yang, Y. Liao and N. Huang, *Biomacromolecules*, 2011, **12**, 1155-1168.
34. W. Kern, *RCA review*, 1970, **31**, 187-206.
35. S. Slavin, A. H. Soeriyadi, L. Voorhaar, M. R. Whittaker, C. R. Becer, C. Boyer, T. P. Davis and D. M. Haddleton, *Soft Matter*, 2012, **8**, 118-128.
36. A. K. Dutta, A. Nayak and G. Belfort, *J. Colloid Interface Sci.*, 2008, **324**, 55-60.
37. N. Weber, H. P. Wendel and J. Kohn, *J. Biomed. Mater. Res. A*, 2005, **72A**, 420-427.
38. A. Domack, O. Prucker, J. Rühe and D. Johannsmann, *Phys. Rev. E*, 1997, **56**, 680.
39. M. V. Voinova, M. Rodahl, M. Jonson and B. Kasemo, *Phys. Scripta.*, 1999, **59**, 391.
40. F. Höök, J. Vörös, M. Rodahl, R. Kurrat, P. Böni, J. Ramsden, M. Textor, N. Spencer, P. Tengvall and J. Gold, *Colloid Surface. B*, 2002, **24**, 155-170.
41. J. Malmstrom, H. Agheli, P. Kingshott and D. S. Sutherland, *Langmuir*, 2007, **23**, 9760-9768.
42. P. Rychter, R. Biczak, B. Herman, A. Smyłła, P. Kurcok, G. Adamus and M. Kowalczuk, Biomacromolecules, 2006, **7**, 3125-3131.
43. K. K. Goli, O. J. Rojas and J. Genzer, *Biomacromolecules*, 2012, **13**, 3769-3779.
44. K. K. Goli, O. J. Rojas, A. E. Oezcam and J. Genzer, *Biomacromolecules*, 2012, **13**, 1371-1382.
45. J. Jin, W. Jiang, J. Zhao, J. Yin and P. Stagnaro, *Appl. Surf. Sci.*, 2012, **258**, 5841-5849.
46. G. M. Liu, Y. Hou, X. A. Xiao and G. Z. Zhang, *J. Phys. Chem. B*, 2010, **114**, 9987-9993.
47. G. B. Sigal, M. Mrksich and G. M. Whitesides, *J. Am. Chem. Soc.*, 1998, **120**, 3464-3473.
48. C. F. Wertz and M. M. Santore, *Langmuir*, 2001, **17**, 3006-3016.
49. L. B. Koh, I. Rodriguez and S. S. Venkatraman, *Biomaterials*, 2010, **31**, 1533-1545.
50. K. Sask, W. McClung, L. Berry, A. Chan and J. Brash, *Acta Biomater.*, 2011.
51. F. Ahmed, N. R. Choudhury, N. K. Dutta, S. Brito e Abreu, A. Zannettino and E. Duncan, *Biomacromolecules*, 2014, **15**, 744-755.
52. D. A. Andrews and P. S. Low, *Curr. Opin. Hematol.*, 1999, **6**, 76.
53. C. Zandén, M. Voinova, J. Gold, D. Mörsdorf, I. Bernhardt and J. Liu, *Eur. Polym. J.*, 2012, **48**, 472-482.
54. C. Cheng, S. Li, S. Nie, W. Zhao, H. Yang, S. Sun and C. Zhao, *Biomacromolecules*, 2012, **13**, 4236-4246.

TOC

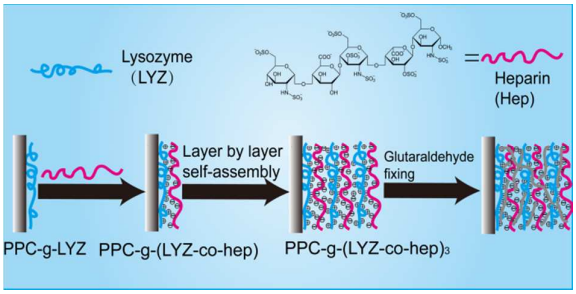

Heparin and lysozyme were used to immobilize onto surface of poly (propylene carbonate) by layer-by-layer assembly to improve hemocompatibility.